Sano *et al.*
Journal of Analytical Science and Technology (2024) 15:24
https://doi.org/10.1186/s40543-024-00438-0

Journal of Analytical Science and Technology

RESEARCH ARTICLE

Open Access

Hf-W dating of zircon in mesosiderite with high-pressure sintered standard

Yuji Sano[1,2*], Yuta Koyama[1], Naoto Takahata[1], Takuya Matsuzaki[2], Mizuho Koike[3], Makiko K. Haba[4], Shuhei Sakata[5], Hideharu Kuwahara[6] and Tetsuo Irifune[6]

Abstract

New standard zircons applicable to in situ analysis of Hf/W ratio by Nanoscale secondary ion mass spectrometer (NanoSIMS) were prepared and applied to Hf-W dating of a differentiated meteorite classified as mesosiderite. The standard zircons were synthesized by high-pressure experiment from starting materials which were mixture of hafnium oxide, tungsten oxide and high-purity zircon powder. The mixed powders were stirred and pulverized by a high-energy ball mill. They were then sintered at 1000 °C and 6 GPa using multi-anvil apparatus. Homogeneity of Hf/W ratios of synthesized zircons was examined by SEM–EDS, EPMA, and Laser Ablation Inductively Coupled Plasma Mass Spectrometer (LA-ICPMS). Hf/W ratios of the same zircons were measured by a NanoSIMS with 2 nA oxygen primary beam and mass resolving power of 10,000. The relative sensitivity factor (RSF) of Hf/W ratio was determined by comparing zircon data measured by LA-ICPMS and NanoSIMS. Observed RSF (Hf/W) of zircon is 0.585 ± 0.180 (hereafter all error 2σ) consistent with 0.855 ± 0.468 of previous work within experimental error margin. The value is higher than observed RSF of glass matrix, 0.301 ± 0.062, and significantly higher than glass data of 0.21–0.22 in references. Based on the RSF, the Hf/W ratios of zircons extracted from mesosiderite "Asuka 882,023" were measured together with W isotopic compositions by NanoSIMS. Observed data in $^{180}Hf/^{186}W$–$^{182}W/^{186}W$ diagram are fitted by a straight line, yielding a slope ($^{182}Hf/^{180}Hf$) of $8.19 \pm 3.50 \times 10^{-6}$. This slope is converted into an absolute zircon Hf-W age of $4536.5^{+4.6}_{-7.2}$ Ma using the age anchor of CV3 chondrite. This age agrees well with a reference value of $4532.0^{+11.4}_{-20.8}$ Ma.

Keywords Standard zircon, High-pressure synthesis, Relative sensitivity factor, Hf-W dating, NanoSIMS

Introduction

Hf-W dating is a chronometer based on the decay of ^{182}Hf to stable ^{182}W with a half-life of 8.9 Myr (Vockenhuber et al. 2004) where ^{182}Hf is called an extinct nuclide, that is, once present at the beginning of the solar system formation but had fully decayed due to its short half-life. Its application to meteoritic zircon ($ZrSiO_4$) is important to discuss the chronology of asteroid accretion, differentiation, and core formation (Burkhardt et al. 2008; Nyquist et al. 2009). However, in situ analysis of Hf/W ratio in zircon shows significant difficulties because there are no natural standard zircons suited for determining the relative sensitivity factor (RSF) of Hf/W ratio. Generally, in SIMS analysis, the difference of the efficiency of ionization (which is called "matrix effect") must be

*Correspondence:
Yuji Sano
ysano@aori.u-tokyo.ac.jp
[1] Atmosphere and Ocean Research Institute, University of Tokyo, Chiba 277-8564, Japan
[2] Marine Core Research Institute, Kochi University, Nankoku 783-8502, Japan
[3] Department of Advanced Science and Engineering, Hiroshima University, Higashihiroshima 739-0046, Japan
[4] Department of Earth and Planetary Sciences, Tokyo Institute of Technology, Tokyo 152-8550, Japan
[5] Earthquake Research Institute, University of Tokyo, Tokyo 113-8654, Japan
[6] Geodynamics Research Center, Ehime University, Matsuyama 790-0825, Japan

corrected with RSF determined with standard materials which contain abundant and homogeneous targeting elements in the same matrix. Nevertheless, natural zircons suitable for RSF determination do not exist due to tungsten's high incompatibility with zircon crystal, namely the Hf/W ratio is 10^4–10^6 in terrestrial zircons (Ireland and Bukovanska 2003).

In previous studies, a few methods were adopted to estimate RSF (Hf/W). Ireland and Bukovanska (2003) used Yb as a proxy for W in zircon, because Yb is a trace element and will behave coherently with other trace elements in the mineral. Srinivasan et al. (2007) adopted the similar protocols when they measured Hf-W age of Eucrite zircon. Koike et al. (2017) used the meteoritic zircon extracted from Agoult of Eucrite group (basaltic rock derived from the crust of 4 Vesta or a similar parent body) as a standard. RSF was estimated by comparing the observed slope of isochron (= ^{182}Hf/^{180}Hf) in a ^{180}Hf/^{186}W-^{182}W/^{186}W diagram and the calculated slope under the assumption that the Hf-W age is identical to its reference ^{207}Pb-^{206}Pb age of 4554.5 Ma (Iizuka et al. 2015). This method is free from matrix effects as the same elements (Hf and W) are measured in the identical matrix (zircon); however, precious meteoric zircons will be consumed in every measurement. To overcome these difficulties, we prepare new standard zircon with known amount of W and Hf. Homogeneity of Hf/W ratio is examined by SEM–EDS, EPMA, and LA-ICPMS. We report RSF (Hf/W) of standard zircon, glass matrix based on the NIST SRM610, and Hf-W age of zircon in a differentiated meteorite.

Material and methods

Synthesizing new standard zircons

High-purity reagent powders (99.9%) of zircon ($ZrSiO_4$ which is Hf free), hafnium oxide (HfO_2), and tungsten oxide (WO_3) were crushed and mixed manually in agate mortar in the proportion for Standard A (Std-A), 1.4% of Hf and 15 ppm of W in weight, and standard B (Std-B), 1.4% of Hf and 1500 ppm in weight, respectively (Table 1). Agate mainly consists of SiO_2 and does not contain appreciable amount of Hf and W. The mixing ratio of both standards has an uncertainty of ± 10%. About 200 mg of powder was taken and further crushed in a grinding jar with ~ 3 g of zirconia beads (5 mm in diameter) for three hours using a high-energy ball mill "Retsch Emax" installed at Geodynamics Research Center (GRC), Ehime University. The beads are made of ZrO_2 and small amounts of Y were added into the product in order to make zirconia mechanically strong. There is no description that W and Hf were incorporated into the beads when they were produced in the factory. The grinding jars are made of stainless steel. There is no apparent description of Hf and W in this stainless steel. A non-negligible amount of mixed powder was stuck to the inner wall of the jars after crushing, so that only 60% of the material was recovered. Figure 1 shows a SEM image of Std-A after crushing by a high-energy ball mill. Size of grain is variable from 0.7 to 2.3 μm with a median value of 1.1 μm. Std-B may have similar characteristics even though no image is available.

A Kawai-type multi-anvil press "ORANGE-3000" (Additional file 1: Fig. S1a) was used to synthesize standard zircons, which was also installed at GRC, Ehime University. A Co-doped MgO octahedral pressure medium with the edge length of 18 mm and tungsten-carbide anvils with the truncation-edge length of 11 mm were used for achieving high pressures. The cell assembly used in synthesis experiments is shown in Additional file 1: Fig.

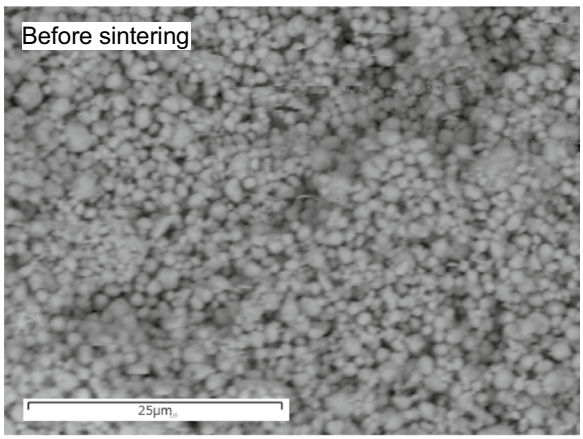

Fig. 1 Scanning electron microscope image of mixed powder of hafnium oxide, tungsten oxide and high-purity zircon (Hf free) before sintering with high-pressure experiment. Bar shows 25 μm

Table 1 Mixed and observed Hf/W ratios of standard zircons

Sample	Mixed			Measured		
	Hf (%)	W (ppm)	Hf/W (molar ratio)	Hf (%)	W (ppm)	Hf/W (molar ratio)
Std-A	1.4	15	933	1.43 ± 0.03	43 ± 6	344 ± 44
Std-B	1.4	1500	9.06	1.53 ± 0.04	1520 ± 230	9.9 ± 1.5

S1b. Crushed and mixed powders were set into a graphite capsule (Additional file 1: Fig. S1b). After the compression at room temperature, high-temperature conditions were achieved by a graphite heater surrounded by ZrO_2 thermal insulator. For synthesis experiments, temperature was estimated from the power–temperature relationship. The powders were sintered at 6 GPa and 1000 ℃ for 3 h. The temperature was controlled to be less than melting point of zircon, because the segregation of W would likely occur in zircon melt. The sintered standards were quenched by turning off the power to the heater and recovered after decompression. Direct contamination by tungsten-carbide anvils may be not likely, because the samples were capsuled by graphite, MgO, graphite, ZrO_2, and then Co-doped MgO (see Additional file 1: Fig. S1b). The recovered zircons and surrounding graphite were embedded on epoxy disk together with a few grains of the NIST SRM610 glass and polished until zircon surface was exposed. Thus, we prepared two synthesized zircon standards (Std-A and Std-B) for NanoSIMS analysis.

Characterization of synthesized zircons

Optical micrographs of synthetic zircon samples after embedding in epoxy resin and surface polishing are shown in Fig. 2. Both samples can be seen encased in graphite and MgO. The small circular spots are traces measured by LA-ICPMS; in Std-A the spots are cross-shaped; and in Std-B they are aligned in a straight line.

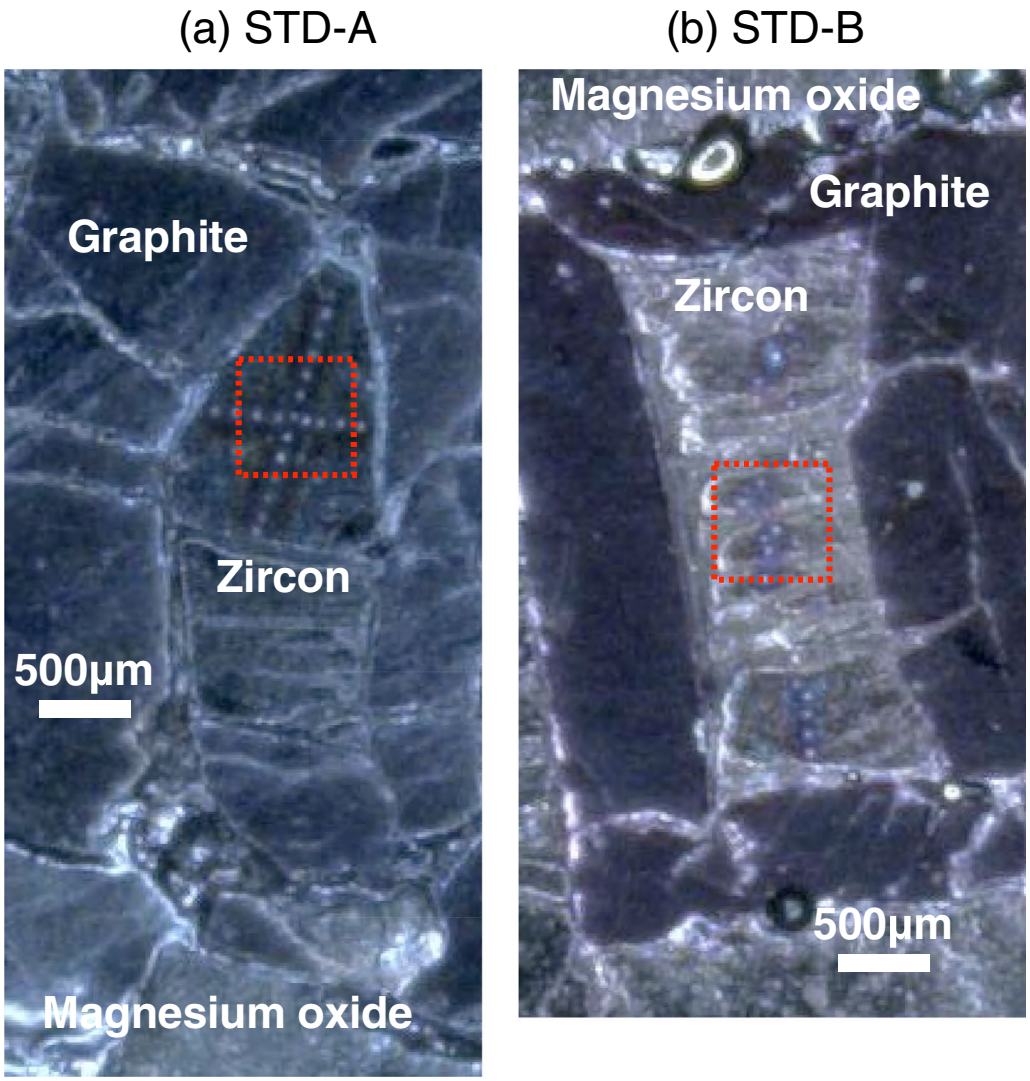

Fig. 2 Optical micrographs of synthetic zircon (Std-A and Std-B) by high-pressure experiments. They were embedded in epoxy resin and the surface was given by mirror finish. The small spots are 20 μm pits carved by LA-ICPMS. Dotted red squares show the areas observed by SEM–EDS in Fig. 3

Both were analyzed by XRD equipment and the results are shown in Additional file 1: Fig. S2. The instrument used was an X'Pert XRD from PANalytical installed at Marine Core Research Institute (MaCRI), Kochi University; the voltage of the X-ray tube was 45 kV and the current value was 40 mA. The anode was made of copper, and the angle of scan was varied from 3° to 75° at 2θ. Since the cross-sectional diameter of the primary X-rays used is about 1–2 cm, the XRD data for both samples are not of zircon alone, but in coexistence with graphite and MgO. Anyway, these results of Std-A and Std-B confirm that the sample sintered at high pressure is zircon crystal by XRD analysis (Additional file 1: Fig. S2).

These samples were then observed by SEM–EDS at MaCRI, Kochi University. The instrument was a Jeol JSM-6500F Field Emission Scanning Electron Microprobe. The acceleration voltage of the primary electrons was 10 keV and the electron beam current was 8×10^{-9} A. The resolution was 3 nm, and the vacuum of the analysis chamber was less than 1×10^{-4} Pa. Figure 3 shows the 330 times magnified images of the area of crossed spots of LA-ICPMS analysis in Std-A (see red dotted rectangle in Fig. 2a), with the SEI image (a) at the top and COMP image (b) at the bottom. The diameter of the LA-ICPMS round pit is 20 μm. The trace analyzed by NanoSIMS is a square where the deposited gold has peeled off and appears charged up and white in the SEI image. The COMP image appears homogeneous as well, with no large voids at this scale.

Figure 3c and d indicates the 330 times magnifications of the central part of Std-B (see red dotted rectangle in Fig. 2b). The SEI image (c) is at the top and the COMP image (d) is at the bottom. The material in this field of view is chemically zircon, but appears to have a different shape; the LA-ICPMS and NanoSIMS pits are located in the targeting areas that appear to be fluffy, and more homogeneous. Additional file 1: Fig. S3-1 is a 1500 times magnification of

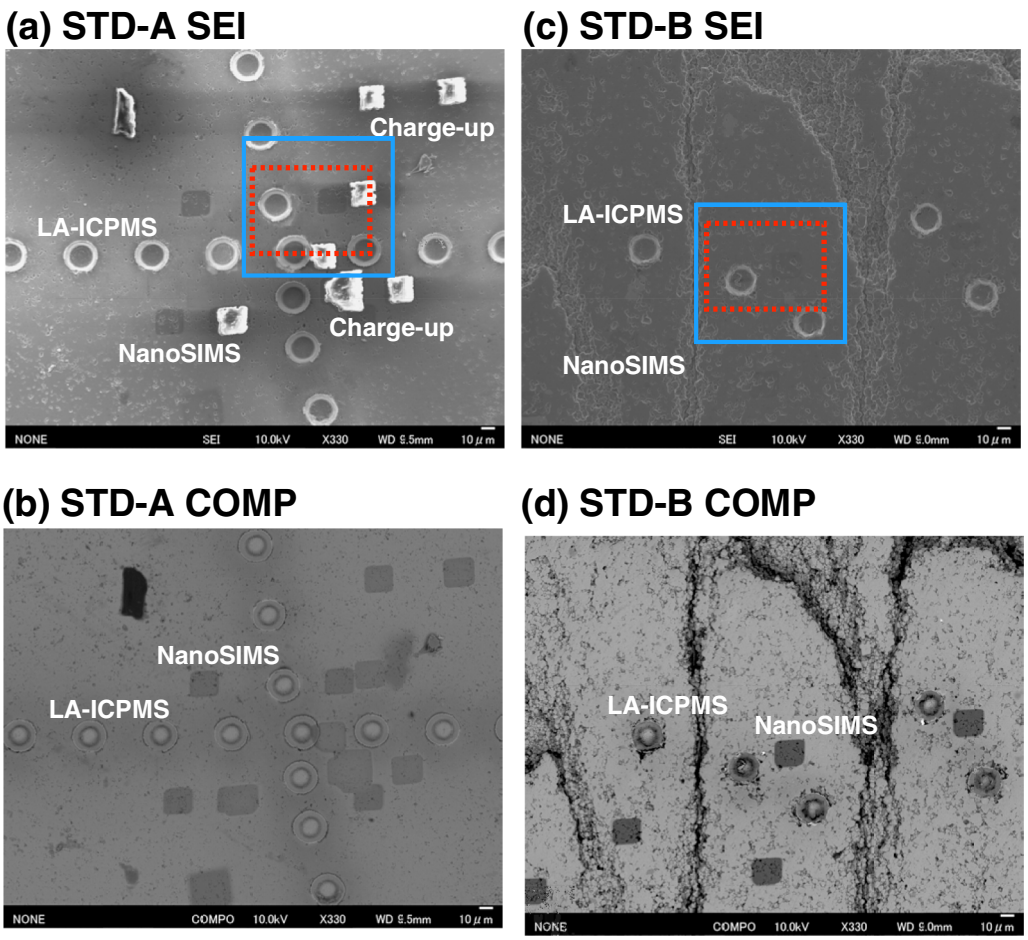

Fig. 3 Scanning electron microscope images of synthetic zircon (Std-A and Std-B) with the 330 times magnification. Bars show 10 μm. **a** SEI image of Std-A, **b** COMP image of Std-A, **c** SEI image of Std-B, **d** COMP image of Std-B. Red dotted and blue solid squares indicate the areas observed by SEM–EDS (Additional file 1: Fig. S3) and EPMA (Fig. 4), respectively

the center of Fig. 3a (dotted rectangle), which is the result of elemental mapping of (b) W, (c) Hf, and (d) Zr by EDS method in addition to SEI image. In the SEI image, some voids can be seen in the NanoSIMS trace squares. The main components, such as Zr and Hf, show no inhomogeneity in the intensity of characteristic X-rays. A few tens of ppm of W are apparently below the detection limit of SEM–EDS.

Additional file 1: Fig. S3-2 is a further enlarged image of the central part of Fig. 3c (red dotted rectangle), and shows the results of elemental mapping of (f) W, (g) Hf, and (h) Zr by EDS method in addition to the SEI image. The SEI image shows large voids in the NanoSIMS trace squares. The concentration of W is about 1500 ppm, but the concentration inhomogeneity may not be visible with the sensitivity of EDS. However, it is clear that there is no inhomogeneity in concentration reaching a few percent. In conclusion, in Std-A and Std-B, there is no heterogeneity in Zr and Hf concentrations, although there are voids of a few μm in size in both cases.

Figure 5-1 shows the elemental mapping of the enlarged blue square in Fig. 4a (Std-A) using an electron probe microanalyzer (EPMA). The instrument used was a JEOL JXA-8200 installed at MaCRI, Kochi University. The acceleration voltage of primary electron was 15 kV, the electron beam intensity was 1×10^{-7} A, and the probe diameter was less than 1 μm. Mapping was done with 1 μm square per pixel and Dwell time was set to 300 ms. Each image consists of 100 pixels × 100 pixels. Except for the squares where Au deposition has been stripped by NanoSIMS analysis and the circular pits by LA-ICPMS, no heterogeneity is visible for all elements (b) W, (c) Hf, and (d) Zr. However, the expected W concentration is 15 ppm, which may be below the detection limit of EPMA.

Figure 5-2 shows the elemental mapping of the enlarged blue square in Fig. 4c (Std-B). Except for the areas where Au deposition has been removed by NanoSIMS analysis and circular pits by LA-ICPMS as in Fig. 5-1, no heterogeneity is seen in (g) Hf and (h) Zr, while (f) W shows 1–3 pixels of enrichment as a tiny nugget. The expected W concentration is about 1500 ppm, and at this concentration, it is possible that the W was not incorporated and/or assimilated into the zircon crystal, but was left behind in the gaps between the microcrystals. The figure also shows that the W-enriched areas are randomly present. Since the NanoSIMS analysis was performed with 20-μm rastering and the LA-ICPMS analysis was performed with a 20-μm-diameter probe diameter, repeated measurements may offset this heterogeneity of W contents.

Analysis of zircons and glass with LA-ICPMS and NanoSIMS

Chemical compositions of synthesized samples were determined by a LA-ICPMS (Agilent 8800) installed at Gakushuin University. Spot analysis with 20 μm diameter was conducted on each zircon to determine the concentrations of Zr, Hf, and W. The observed data were calibrated against NIST SRM 610 standard glass, whose major and trace element abundances have been well documented (Jochum et al. 2011). Twenty-one and thirteen spots were analyzed to check the homogeneity of targeting elements in Std-A and Std-B, respectively. Observed Hf/W ratio of zircon samples was calibrated against that of NIST SRM 610 glass, under the assumption that the matrix effect of LA-ICPMS is small (Halter and Heinrich 2004).

The measurement of Hf/W ratio and W isotopic composition in synthesized and meteoritic zircons together with the NIST SRM610 glass was carried out by a Cameca NanoSIMS ion microprobe installed at Atmosphere and Ocean Research Institute (AORI), the University of Tokyo. 2 nA O^- primary ion beam was used (spot size: 7 μm) with rastering by 20 × 20 μm, resulting 20 μm rectangular pits formed (here after called raster-mode). Mass resolving power was set approximately 10,000 to separate ^{186}W from $^{170}Yb^{16}O$ (Additional file 1: Fig. 4). Secondary ions of $^{30}Si^+$, $^{96}Zr^{16}O_2^+$, $^{178}Hf^+$, $^{186}W^+$, $^{186}W^{16}O^+$ were acquired simultaneously, and $^{182}W^+$ and $^{183}W^+$ were counted by the same detector as $^{186}W^+$ by a magnetic field switching (Additional file 1: Table S1). Counting time of each ion was 1000 s in total (10 s/cycle × 100 cycles). Further experimental details are given by Koike et al. (2017). All of analyzed spots on standard zircons by NanoSIMS were located close to those by LA-ICPMS (see Fig. 3).

Meteoritic samples

Mesosiderites are differentiated meteorites composed of silicates and Fe–Ni metals, and they are classified into four groups based on metamorphic degrees. Asuka 882,023 is found in Antarctic and belongs to mesosiderite of type 2/3A with considerably thermally metamorphosed signature. We have extracted five zircon grains from the meteorite by acid leaching in the same manner as a previous study (Haba et al. 2019). They were embedded on resin and the surface was polished until mid-section was exposed. All grains were approximately 40–60 μm in diameter (Fig. 6) and there are no growth bands and heterogeneous bright pattern by a cathode luminescence observation.

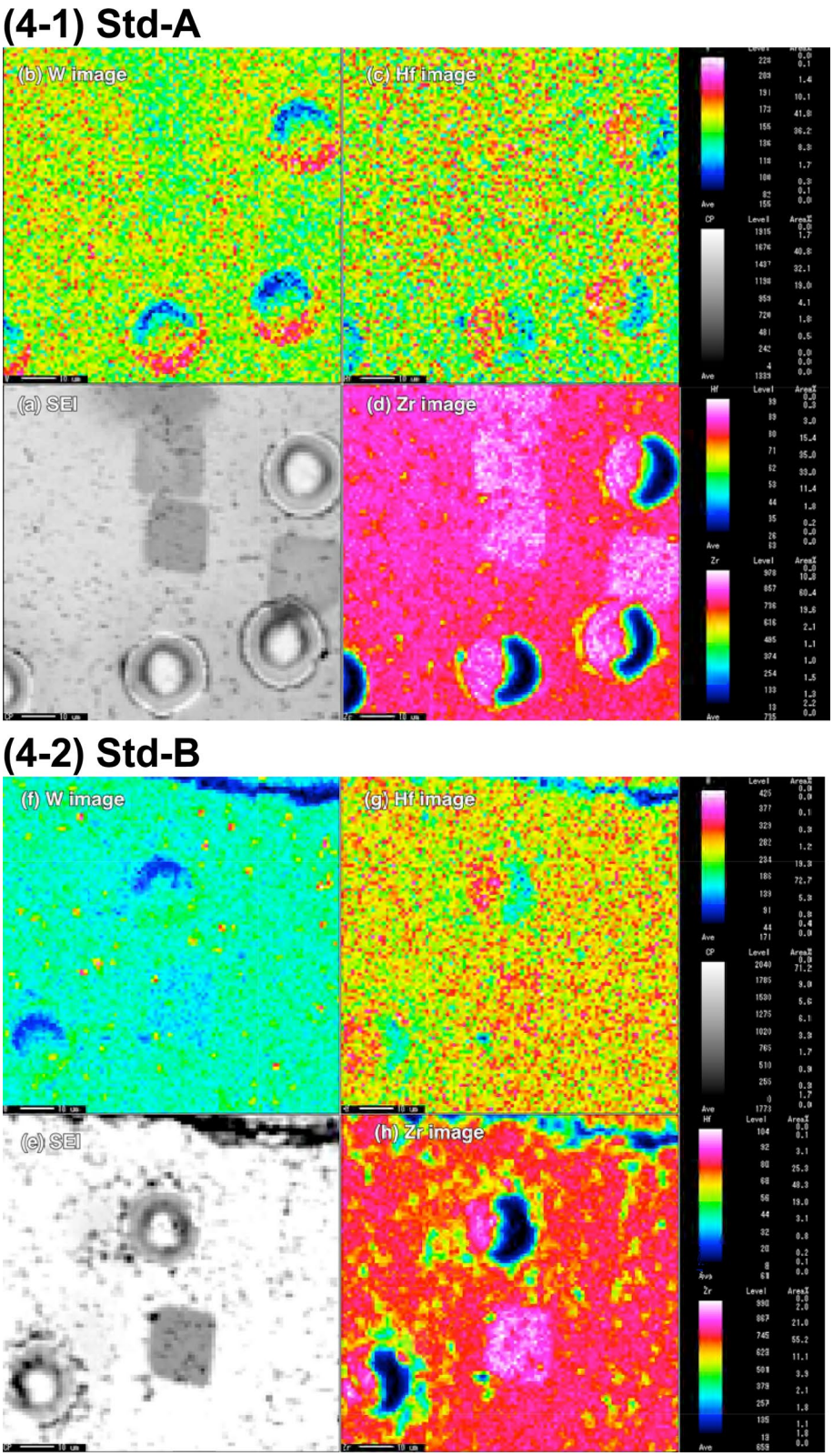

Fig. 4 Electron probe microanalyzer images of synthetic zircon. (4–1) Enlarged images of Std-A for the blue square area in Fig. 3a. **a** SEI image, **b** W image, **c** Hf image, and **d** Zr image. (4–2) Enlarged images of Std-B for the blue square area in Fig. 3c. **e** SEI image, **f** W image, **g** Hf image, and **h** Zr image. Bars show 10 μm

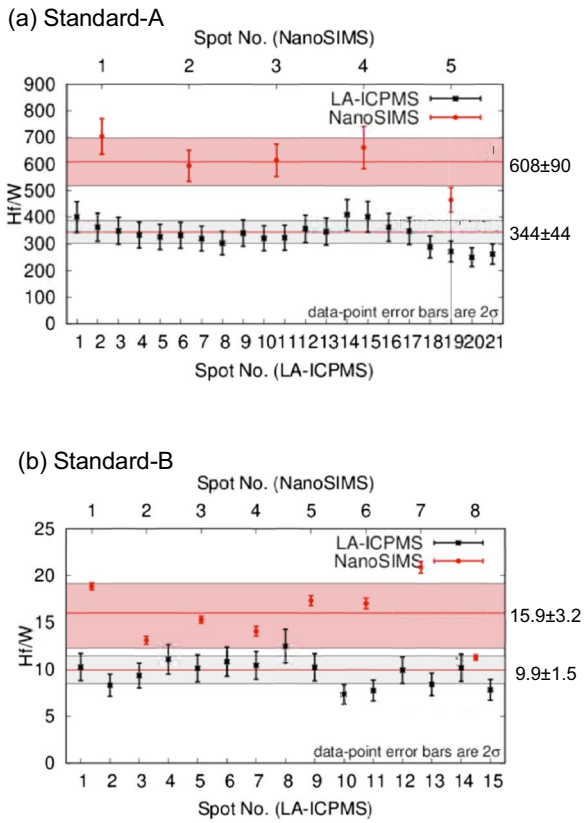

Fig. 5 Comparison of Hf/W ratios measured by LA-ICPMS and NanoSIMS in sintered zircon standard. **a** Observed data for standard A. Mixing ratio of Hf/W was 933, while the measured ratio was 344, suggesting a W contamination. Bars show 2σ errors. NanoSIMS data are larger than those of LA-ICMPS. **b** Observed data for standard B. Mixing ratio of Hf/W is 9.06. LA-ICPMS data are consistent with the mixing ratio. Bars show 2σ errors. NanoSIMS data are again larger than those of LA-ICMPS

Results and discussion

Synthesized standard zircons

Observed elemental Hf/W ratios of Std-A zircon vary from 258 to 421 with the average of 344 ± 88 (hereafter all error 2σ) by 21 spot analysis using LA-ICPMS (Additional file 1: Table S2). This value is much smaller than the molar mixing ratio of 933. There may be unknown source of W in the sample, extra W of 28 ppm, possibly due to the contamination by a high-energy ball mill. There is no apparent description of W incorporated either in zirconia beads or the stainless steel grinding jars. However, observed result suggests the contamination during the grinding procedure may have occurred. Although this result is due to a lack of experimental attention, if the Hf/W ratio is homogeneous at a few microns in size and accurately obtained, it is judged to be acceptable as a standard sample. Observed Hf/W ratios of Std-B are ranging from 7.56 to 12.86 with the average of 9.9 ± 3.0 (hereafter all error 2σ). This value agrees with the molar mixing ratio of 9.06 (Table 1). This standard contains a lot of initial W, approximately 1500 ppm, contaminant of 28 ppm may be negligible and well within experimental error margin. On the other hand, there is a heterogeneity of W contents observed by EPMA mapping (Fig. 4-2f). The round pit of LA-ICMPS is approximately 20 μm diameter and larger than the W-enriched nuggets with 1–3 μm. Each pit may have a similar number of W nuggets by chance and may show the similar Hf/W ratio.

Observed elemental Hf/W ratios of Std-A by NanoSIMS are summarized in Additional file 1: Table S3. The Hf/W ratio of Std-A varies from 479 to 725 with the average of 608 ± 180 by raster-mode 5 individual analyses. Data are simply measured intensity ratio of Hf and W ion beams of NanoSIMS. Observed Hf/W ratio of Std-B is ranging from 11.6 to 21.5 with the average of 9.9 ± 3.0 by raster-mode 8 individual analyses. Raster area of NanoSIMS is 20 μm square and larger than the size of W-enriched nuggets. Again the each raster area may have a similar number of W nuggets by chance and may show the similar Hf/W ratio. Thus, repeated analysis may offset the heterogeneity of W in Std-B.

Relatively sensitivity factor of Hf/W ratio

In this study, we define relative sensitivity factor of Hf and W ratio in NanoSIMS raster-mode analysis; RSF(Hf/W) as follows:

$$\mathrm{RSF(Hf/W)} = \frac{\left(^{180}\mathrm{Hf}/^{186}\mathrm{W}\right)_{\mathrm{true}}}{\left(^{180}\mathrm{Hf}/^{186}\mathrm{W}\right)_{\mathrm{NanoSIMS}}} \quad (1)$$

where $\left(^{180}\mathrm{Hf}/^{186}\mathrm{W}\right)_{\mathrm{true}}$ and $\left(^{180}\mathrm{Hf}/^{186}\mathrm{W}\right)_{\mathrm{NanoSIMS}}$ are true ratio and measured value of $^{180}\mathrm{Hf}/^{186}\mathrm{W}$ ratio by NanoSIMS. In the case of glass matrix, true value is derived from reference data (Jochum et al. 2011). On the other hand, true value is based on those measured by LA-ICMPS in zircon matrix.

In the case of glass matrix, we measured $^{182}\mathrm{W}/^{186}\mathrm{W}$ and $^{178}\mathrm{Hf}/^{186}\mathrm{W}$ ratios of NIST SRM610 glass standard by raster-mode. Data of repeated analysis are listed in Table 2. Observed $^{182}\mathrm{W}/^{186}\mathrm{W}$ ratios vary from 0.883 to 1.07 with the average of 0.943 ± 0.140, which is consistent with the recommended value of 0.9321 within experimental error margin by IUPAC Technical Report (De Laeter et al. 2003). Observed $^{178}\mathrm{Hf}/^{186}\mathrm{W}$ ratios are converted into $^{180}\mathrm{Hf}/^{186}\mathrm{W}$ ratios based on the $^{180}\mathrm{Hf}/^{178}\mathrm{Hf}$ ratio of 1.2859 (De Laeter et al. 2003). They are ranging from 3.37 to 4.54 with the average of 4.14 ± 0.86. On the other hand, Hf and W concentrations of NIST SRM 610 glass are 435 ppm and 444 ppm, respectively, by recommended values (Jochum et al. 2011). Assuming their isotopic abundances, the true $^{180}\mathrm{Hf}/^{186}\mathrm{W}$ ratio becomes 1.2472, which is much smaller than the ratio of 4.14

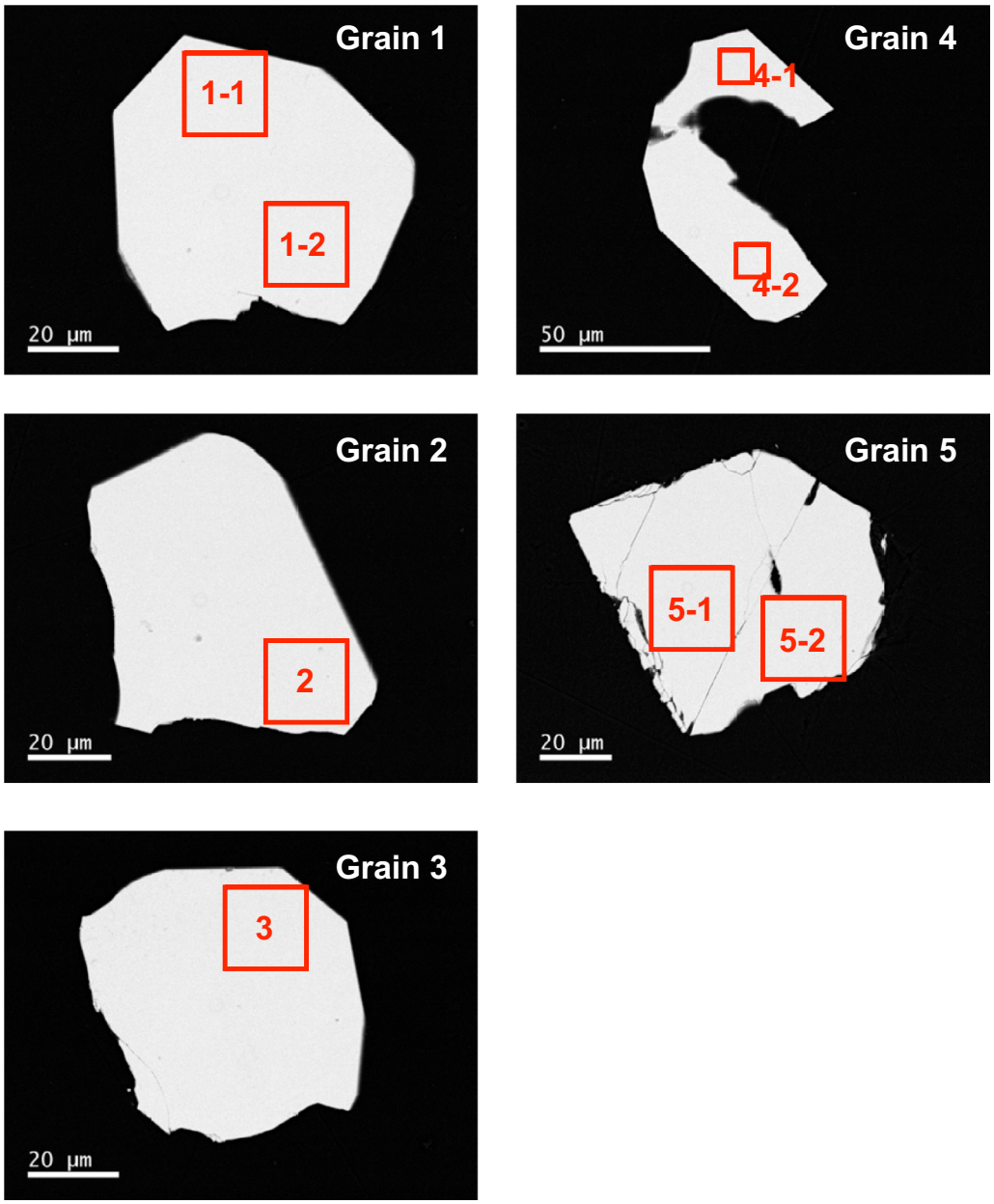

Fig. 6 Scanning electron microscope image of zircon grains extracted from mesosiderite "Asuka 882,023." Bars show 20μm or 50 μm. Based on the image, inclusion-free homogeneous regions suitable for NanoSIMS analysis were located by eyes and shown by red squares

measured by NanoSIMS. It is possible to calculate the RSF(Hf/W) by an apparent ratio of 1.2472/4.14 = 0.301. There are two RSF data of glass matrix available in studies (Ireland and Bukovanska 2003; Srinivasan et al., 2007) and listed in Table 3. Estimated value of 0.301 ± 0.062 in this work is larger than reference values of 0.220 ± 0.008 and 0.21 ± 0.02. It is difficult to explain the difference, because previous researches used the same SRM610 glass. The discrepancy may be derived from the ionization efficiency due to analytical mode of SIMS, where reference data were obtained by a spot analysis, while our data by raster-mode. This should be clarified in a future work.

Figure 5 shows visualized data of two synthesized zircon standard (Std-A and B) measured by LA-ICPMS and NanoSIMS. In the case of Std-A, true value of Hf/W ratio is 344 ± 88 analyzed by LA-ICPMS, while observed Hf/W ratio is 608 ± 180 by NanoSIMS. Then, RSF (Hf/W) becomes 0.566 ± 0.222 based on Eq. (1). In the case of Std-B, both Hf/W ratios are 9.9 ± 3.0 and 15.9 ± 6.4

Table 2 $^{182}W/^{186}W$ and $^{180}Hf/^{186}W$ ratios of NIST SRM610 glass

No.	$^{182}W/^{186}W$		2σError*	$^{180}Hf/^{186}W$
1	0.890	±	0.020	4.54
2	0.933	±	0.018	3.37
3	1.070	±	0.020	4.33
4	0.973	±	0.018	3.93
5	0.907	±	0.012	4.31
6	0.883	±	0.018	4.39
Ave.	0.943			4.14
Std.	0.140			0.43

*The error is estimated by a standard deviation of 100 data set of 182W/186W ratio measured by NanoSIMS

Table 3 Relative sensitivity factor (Hf/W) of glass and zircon matrix

Instrument	Matrix	RSF (Hf/W)	Error (2σ)	References
SHRIMP	Glass	0.220	0.008	Ireland and Bukovanska (2003)
IMS 1270	Glass	0.21	0.02	Srinivasan et al. (2007)
NanoSIMS	Glass	0.301	0.062	This work
SHRIMP	Zircon	0.286	0.020	Ireland and Bukovanska (2003)
NanoSIMS	Zircon	0.855	0.468	Koike et al. (2017)
NanoSIMS	Zircon	0.585	0.180	This work

by LA-ICPMS and NanoSIMS, respectively, and RSF be 0.623 ± 0.314. As stated in the former section, W is located heterogeneously in Std-B (Fig. 4-2). However, the 1–3 microns W nuggets are smaller than the probe area of LA-ICMPS and NanoSIMS. In the case of LA-ICPMS, tiny W nuggets are ablated together with zircon matrix materials and introduced into the ion source of ICP and ionized immediately. Consequently, there may be no difference between the homogeneous (Std-A) and heterogeneous (Std-B) distribution of W in the sample by LA-ICPMS. In the case of NanoSIMS, it is difficult to consider the ionization process of mixed materials within the raster area. Since the RSF (Hf/W) of Std-A is similar to that of Std-B where W nuggets exist in it, the overall sensitivity and ionization efficiency of homogeneous and heterogeneous samples may be comparable. Further explanation is well beyond the scope of this work and will be verified in future work.

Combining these two data of Std-A and B by error weighted mean, the RSF (Hf/W) of zircon matrix is 0.585 ± 0.180 obtained in this work (Table 3). This value is much larger than the RSF of glass matrix, 0.301 ± 0.062, suggesting that there is certainly matrix effect in NanoSIMS analysis. On the other hand, the zircon RSF of 0.585 ± 0.180 is consistent with a reference value of 0.855 ± 0.468 estimated by an indirect way, even though under the identical matrix (Koike et al. 2017) and higher that the value of 0.286 ± 0.020 by Ireland and Bukovanska (2003).

Hf-W dating of Asuka 882,023 zircon

We have measured $^{182}W/^{186}W$ and $^{180}Hf/^{186}W$ ratios of 5 zircon grains extracted from mesosiderite, Asuka 882,023. For Grain#1, #4, and #5, two raster-mode analyses were conducted at different area on the surface, while for Grain#2 and #3, single measurement was carried out (Fig. 6). Observed Hf-W data of eight analyses are listed in Table 4 together with error correlation, ρ of $^{182}W/^{186}W$ and $^{180}Hf/^{186}W$ ratios, which is constrained by a small counting rate of ^{182}W and ^{186}W and calculated by 100 cycles data set. The $^{182}W/^{186}W$ ratio vary significantly from 1.06 to 4.21 with the average of 2.36 ± 1.92 (2σ), which is comparable to that of 0.93170 ± 0.00002 in a metal part of mesosideraite (Quitte et al. 2005). Excess ^{182}W in these sample is possibly attributable to decay product of extinct nuclide, ^{182}Hf, which was available in early solar system (Kleine et al. 2004). However, this value alone does not provide an exact age. Its relation to elemental ratio of Hf/W is needed. Observed $^{180}Hf/^{186}W$ ratios are listed in Table 4, where these values were corrected by zircon RSF (Hf/W) observed in this work. The $^{180}Hf/^{186}W$ ratios vary significantly from 6.13×10^4 to 2.43×10^5 with the average of 15.6×10^5, which is similar to those of terrestrial zircons (Ireland and Bukovanska 2003) and meteorite zircons (Srinivasan et al. 2007).

Figure 7 indicates a relationship between observed $^{180}Hf/^{186}W$ and $^{182}W/^{186}W$ ratios of Asuka 882,023 zircons. There is a positive correlation between them, even though data are scattering. Error assigned to the ratio is 1σ value. This relation is called isochron. A line approximation using the York method (calculated by Isoplot 4.15), which accounts for errors in both axes,

Table 4 W isotopic ratios and Hf/W ratios of zircon in mesosiderite

Sample	$^{182}W/^{186}W$	$^{183}W/^{186}W$	$^{180}Hf/^{186}W$	*P*
Grain#1–1	2.00 ± 1.03	0.80 ± 0.58	$(11.2\pm5.0)\times10^4$	0.82
Grain#1–2	3.25 ± 1.57	1.50 ± 1.07	$(22.2\pm10.4)\times10^4$	0.95
Grain#2	2.08 ± 0.57	2.24 ± 1.34	$(6.13\pm1.62)\times10^4$	0.71
Grain#3	2.44 ± 1.53	2.93 ± 1.01	$(23.2\pm12.8)\times10^4$	0.88
Grain#4–1	1.27 ± 0.39	1.08 ± 0.73	$(4.72\pm1.22)\times10^4$	0.64
Grain#4–2	4.21 ± 1.56	1.69 ± 1.07	$(24.3\pm9.2)\times10^4$	0.94
Grain#5–1	1.06 ± 1.03	2.67 ± 1.82	$(14.7\pm10.4)\times10^4$	0.79
Grain#5–2	2.58 ± 1.59	1.82 ± 1.14	$(18.6\pm10.7)\times10^4$	0.93

Error assigned to the ratio is one sigma

P shows error correlation between $^{182}W/^{186}W$ and $^{180}Hf/^{186}W$ ratio

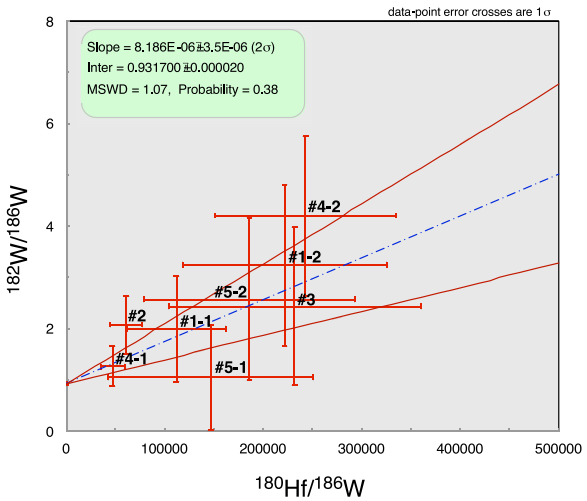

Fig. 7 A correlation diagram between $^{180}Hf/^{186}W$ and $^{182}W/^{186}W$ ratios of mesosiderite "Asuka 882,023" zircons. Error bars assigned to data point are 1σ. Blue and red lines are isochron and 95% confidence interval, respectively. A line approximation was made by accounting errors in both axes using Isoplot 4.15

yields a line with a slope of $(8.19 \pm 3.50) \times 10^{-6}$ (2σ error, MSWD = 1.07), where the regression is constrained to $^{182}W/^{186}W$ ratio of 0.93170 ± 0.00002 at Y-intercept based on the calculation of Koike et al. (2017) and W isotopes of mesosiderite metal (Quitte et al. 2005). This slope ($^{182}Hf/^{186}Hf$ ratio) would provide a relative age to any anchor sample with a half-life of 8.9 Myr (Vockenhuber et al. 2004). If we adopt the anchor of Ca, Al-rich inclusions (CAIs) from CV3 chondrites, where the $^{182}Hf/^{186}Hf$ ratio and absolute age are $(9.72 \pm 0.22) \times 10^{-6}$ and 4568.3 ± 0.7 Ma (Burkhardt et al. 2008), the observed slope of mesosiderite is converted into an absolute age of $4536.5^{+4.6}_{-7.2}$ Ma under the assumption that initial $^{182}Hf/^{186}Hf$ ratio of mesosiderite parent body is the same as that of CV3 chondrite. This age is consistent with previous Hf-W age of $4532.8^{+11.4}_{-21.0}$ Ma (Koike et al. 2017). Concerning of chronology of asteroid 4 Vesta, Haba et al. (2019) reported two important events; initial crust formation at 4558.5 Ma and hit-and-run collision at 4525.4 Ma based on precise ^{207}Pb-^{206}Pb ages of five mesosiderites (Vaca Muerta, NWA1242, NWA8402, Estherville, and NWA8741). Observed Hf-W age of 4536.9 Ma in this work is between them and may be unknown event on Vesta. However, further discussion is out of scope of present study, because no precise ^{207}Pb-^{206}Pb age of Asuka 882,023 is available in studies.

Conclusion

To accurately determine the Hf-W age of zircon in meteorites using secondary ion mass spectrometer (SIMS), we have artificially synthesized homogeneous standard zircons containing sufficient amounts of W under high-temperature and pressure conditions. The zircons were analyzed repeatedly at multiple points by LA-ICPMS and NanoSIMS to determine the relative sensitivity factor (RSF) of Hf and W. The estimated value of 0.585 ± 0.180 is consistent with a literature value of 0.855 ± 0.468 for the same matrix. This value was used to determine the Hf-W age of zircons extracted from a differentiated meteorite classified as mesosiderite (Asuka 882,023). The result was $4536.5^{+4.6}_{-7.2}$ Ma, which agrees with previous study of $4532.8^{+11.4}_{-21.0}$ Ma within error. The standard zircons will be useful for future Hf-W dating using SIMS instruments.

Supplementary Information

The online version contains supplementary material available at https://doi.org/10.1186/s40543-024-00438-0.

Additional file 1. Supplementary figures and tables.

Acknowledgements

We thank Naoji Sugiura for stimulating us into this study and Chang-sik Cheong, Hiroshi Hidaka, and Yuri Amerin for providing us chance to submit this study.

Author contributions

YS conceived and designed the project. YK, HK, and TI conducted high-pressure experiment. SS obtained LA-ICPMS data. MT performed XRD, SEM–EDS, and EPMA analysis. YK, NT, and MK carried out NanoSIMS analysis. MKH provided mesosiderite zircon samples. YK and YS wrote the paper with comments and improvements from all authors.

Funding

Grant-in-Aid for Scientific Research (Kaken) 19H00726 and 20K20937. Research Grants in the Natural Sciences of Mitsubishi Zaidan 202010023.

Availability of data and materials

All data for this study are available from the corresponding author on request.

Declarations

Competing interests

The authors declare that they have no competing interests.

Received: 1 October 2023 Accepted: 11 April 2024
Published online: 23 April 2024

References

Burkhardt C, Kleine T, Bourdon B, Palme H, Zipfel J, Friedrich JM, Ebel DS. Hf–W mineral isochron for Ca, Al-rich inclusions: age of the solar system and the timing of core formation in planetesimals. Geochim Cosmochim Acta. 2008;72:6177–97.

De Laeter JR, Bohlke JK, De Bievre P, Hidaka H, Peiser HS, Rosman KJR, Taylor PDP. Atomic weights of the elements: review 2000. Pure Appl Chem. 2003;75:683–800.

Haba MK, Wotzlaw J-K, Lai Y-J, Yamaguchi A, Schönbächler M. Mesosiderite formation on asteroid 4 Vesta by a hit-and-run collision. Nat Geosci. 2019;12:510–5.

Halter WE, Pettke T, Heinrich CA. Laser-ablation ICP-MS analysis of silicate and sulfide melt inclusions in an andesitic complex I: analytical approach and data evaluation. Contrib Mineral Petrol. 2004;147:385–96.
Iizuka T, Yamaguchi A, Haba MK, Amelin Y, Holden Y, Zink S, Huyskens MH, Ireland RT. Timing of global crustal metamorphism on Vesta as revealed by high-precision U-Pb dating and trace element chemistry of eucrite zircon. Earth Planet Sci Lett. 2015;409:182–92.
Ireland TR, Bukovanska M. Initial $^{182}Hf/^{180}Hf$ in meteoritic zircons. Geochim Cosmochim Acta. 2003;67:4849–56.
Jochum KP, Weis U, Stoll B, Kuzmin D, Yang Q, Raczek I, Jacob DE, Stracke A, Birbaum K, Frick DA, Günther D, Jacinta Enzweiler J. Determination of reference values for NIST SRM 610–617 glasses following ISO guidelines. Geostand Geoanal Res. 2011;35:397–429.
Kleine T, Mezger K, Munker C, Palme H, Bishoff A. ^{182}Hf-^{182}W isotope systematics of chondrites, eucrites, and martian meteorites: chronology of core formation and early mantle differentiation in Vesta and Mars. Geochim Cosmochim Acta. 2004;68:2935–46.
Koike M, Sugiura N, Takahata N, Ishida A, Sano Y. U-Pb and Hf-W dating of young zircon in mesosiderite Asuka 882023. Geophys Res Lett. 2017;44:1251–9.
Nyquist LE, Kleine T, Shih C-Y, Reese YD. The distribution of short-lived radioisotopes in the early solar system and the chronology of asteroid accretion, differentiation, and secondary mineralization. Geochim Cosmochim Acta. 2009;73:5115–36.
Quitte G, Birck J-L, Allegre CJ. Stony-iron meteorites: history of the metal phase according to tungsten isotopes. Geochim Cosmochim Acta. 2005;69:1321–32.
Srinivasan G, Whitehouse MJ, Weber I, Yamaguchi A. The crystallization age of eucrite zircon. Science. 2007;317:345–7.
Vockenhuber C, Oberli F, Bichler M, Ahmad I, Quitte G, Meier M, Halliday AN, Lee D-C, Kutschera W, Steier P, Gehrke PR, Helmer RG. New half-life measurement of 182hf: improved chronometer for the early solar system. Phys Rev Lett. 2004;93: 172501.

Publisher's Note